
Article:
Shu, A., Wang, L., Shao, S. et al. (1 more author) (2017) Study on two-phase dynamic behaviours within non-homogeneous debris flow. Proceedings of the ICE - Water Management, 171 (6). pp. 283-298. ISSN 0020-3262

https://doi.org/10.1680/jwama.16.00072

Investigation on dynamic behaviours of liquid and solid phases within non-homogeneous debris flows

Anping Shu[1], Le Wang[2]*, Songdong Shao[3,4] and Guoqiang Ou[5]

[1] Professor, School of Environment, Key Laboratory of Water and Sediment Sciences of MOE, Beijing Normal University, Beijing 100875, China. E-mail: shuap@bnu.edu.cn

[2] Postdoctoral Researcher, State Key Laboratory of Hydroscience and Engineering, Tsinghua University, Beijing 100084, China. Email: lewang2016@mail.tsinghua.edu.cn

[3] Senior Lecturer, Department of Civil and Structural Engineering, University of Sheffield, Sheffield S1 3JD, UK. E-mail: s.shao@sheffield.ac.uk

[4] Visiting Professor, State Key Laboratory of Hydroscience and Engineering, Tsinghua University, Beijing 100084, China.

[5] Professor, Institute of Chengdu Mountain Hazard and Environment, Chinese Academy of Sciences, Chengdu 610000, China. E-mail: ougq@imde.ac.cn

* Corresponding author

Abstract

The non-homogeneous debris flows, consisting of a wide range of grain size, bulk density and demonstrating non-uniform velocity distributions, are commonly modeled as the two-phase flow. In adopting such an approach, a critical grain diameter to separate the solid and liquid phase, within such debris flows, can be determined through the principles of minimum energy dissipation. In the current study, an improved analytical approach using the resistance formula of water flow and mass conservation law is presented to determine the velocity of the solid and liquid phases within a non-homogeneous debris flow, based on the derived critical grain diameter. Some of the dynamic parameters required in the analysis are validated against the experimental data of a non-homogeneous, two-phase debris flow measured from the Jiangjia gully, Yunnan Province of China. The results show that, for the majority of non-homogeneous debris flows tested, the liquid phase exhibits higher velocity than the solid phase. However, as the bulk density of the debris flow increases, the solid phase tends to have higher velocity than the liquid phase. These findings are shown to have important implications on the vertical grading patterns of the bed deposits in depositional areas. The observations from the field studies indicate that the non-homogeneous debris flows with bulk density being significantly lower, close to and significantly higher than the critical value seem to exhibit normal (i.e. bed-to-surface vertical fining), mixed, and inverse (bed-to-surface vertical coarsening) grading patterns in the alluvial fan deposits.

Keywords: non-homogeneous debris flow; two phase; bulk density; vertical grading; critical diameter; Jiangjia gully

1. Introduction

Debris flows arise from the destabilization of a mass of poorly-sorted, water-saturated sediments, which leads to a flow-like propagation due to the gravitational acceleration (e.g.,

landslides). Within such flows, both the solid and fluid forces are known to influence the motion (Iverson, 1997a), with the resulting velocity profile distribution often being similar to that of the fluid flows (Hungr, 1995). Debris flows are typically classified as the muddy, non-homogeneous and water-borne flows, on the basis of their compositions (e.g., fine- or coarse-grained) and the bulk density of solid materials contained within the mixture (Ancey, 2001). Fine particles, such as silt and clay, are the main component of muddy flows, while coarser particles, such as large cobbles, constitute the main component of water-borne debris flows. For the non-homogeneous debris flows in present study, the solid phase consists of coarse particles ranging in size from sand to large cobble, while the liquid phase is composed of the water containing fine clay or silt. Under this condition, both the fine and coarse particles play an important role in the composition and dynamic flow process.

A number of mathematical models have been developed to simulate the debris-flow behaviours (Takahashi, 1978, 1980; Savage and Hutter, 1989; Iverson, 1997a, 1997b; Fraccarollo and Papa, 2000; Iverson and Vallance, 2001; Pitman and Le, 2005; Patra et al., 2005; Sheridan et al., 2005; Rickenmann et al., 2006; Williams et al., 2008). Generally, single-phase models have been applied to both the muddy and the water-borne debris flows. For example, Takahashi (1978; 1980) proposed a model that is applicable to the water-borne debris flows, in which a dilatant model was used. Similarly, a more advanced TRENT-2D model developed by Armanini et al. (2009) is more suitable for the debris flows with coarser (cohesionless) materials composed of solid fraction and negligible viscosity assumed for the interstitial fluid (Armanini et al., 2009; Armanini et al., 2014; Stancanelli and Foti, 2015; Rosatti et al., 2015), this model was fundamentally characterized by the mass exchange between erodible bed and debris flow. In the FLO-2D model given by Brien and Julien (1985), it was assumed that a debris flow acts as a homogeneous Bingham fluid (Stancanelli and Foti, 2015), and this model is better suited to describe the debris flows characterized by fine sediments (e.g. hyper-concentrated sediment flows), and the SHALSTAB model proposed by Montgomery et al. (1994) was normally used to study the slope stability and more relevant to the shallow landslide. Likewise, the TITAN2D models (Savage and Hutter, 1989; Patra et al., 2005; Sheridan et al., 2005; Williams et al., 2008) were established based

upon the incompressible Coulomb continuum law, and they are specifically applicable to the fine-grained muddy flows (such as volcano and avalanche event). In contrast, the two-phase flow models, which treat the solid and liquid phases of the debris flow separately, are found to be more suitable for the simulation of non-homogeneous debris flows (Pitman and Le, 2005; Shu et al., 2008, and 2010). There are two main challenges, however, found in the practical applications of these two-phase modeling approaches.

The first challenge is the determination of the critical grain size d_0 that is used to separate the liquid and solid phases within the non-homogeneous debris flows. Although it is relatively easy to qualitatively define the fluid phase as being composed of the water and fine sediments less than the critical grain size d_0, with the solid phase consisting of grain sizes larger than d_0, it is much more difficult to quantify this in reality (Xiong, 1996). In the previous studies, a constant critical value of d_0 = 2.0 mm (Xiong, 1996) was utilized due to the limitation of the rheological instruments, while other studies adopting approaches such as the yield stress method (Xiong, 1996) led to the unrealistic d_0 values. More recently, Shu et al. (2008) introduced a minimum energy dissipation modelling approach to determine d_0 for the experimental debris flows in the Jiangjia gully of Yunnan Province, China. Their results implied that the critical diameter d_0 could vary for the different types of the debris flows, but within a predicted range of 4.0 mm – 7.0 mm, which coincides with the reported sediment grain size separating the bed load (i.e. coarse sediment) and suspended load (i.e. fine sediment) of the non-homogeneous debris flows (Wu et al., 1993; Wang and Qian, 1987; Takahashi, 2007; Yang et al., 2014).

The second challenge relates to the availability and complexity of two-phase debris flow models (Shu et al., 2010). The majority of two-phase flow models lose some kinds of the advantage over the single-phase models due to the assumption of negligible velocity difference between the liquid and solid phases when solving the momentum equations. Although several models are theoretically equipped with the capability of determining the velocity differences, they are too complex to be solved and validated by the experimental dataset (Martinez, 2009). In addition, most of these two-phase models can only be applied

under very strict parametric conditions, which is quite far away from the practical purpose (Martinez, 2009). The above-mentioned limitations mean that the transport and deposition dynamics of non-homogeneous debris flows are still poorly understood, especially the relative behaviour of (and the interactions between) fluid and solid phases, as well as how this is influenced by the composition and bulk density of the debris flows. The present study aims to address these knowledge gaps (i.e. the determination of critical grain size and understanding of the dynamic properties of liquid and solid phases within non-homogeneous debris flows) through the analysis of both experimentally-generated and naturally-observed debris flows.

Traditionally, the debris-flow deposits have been commonly observed to demonstrate: (i) normal grading; (ii) disorderly/mixed grading; and (iii) inverse grading of their coarsest fragments in the vertical structure (Naylor, 1980; Major, 1994 and 1997; Wang, 2009; Starheim et al., 2013). However, these findings are typically restricted to the post-event analysis and used to infer information on the physical properties of debris flow, which is highly questionable since the accumulation of sediments could potentially be induced by a discrete pulse of single flow or an individual flow (Major, 1997). As a result, very few investigations have linked direct observations of the flow behaviour and depositional process of a single debris-flow event to the characteristics of the corresponding deposits (e.g., Suwa and Okuda, 1983; Major, 1997). As such, this paper considers a physically-simplified, two-phase flow model that could tentatively reveal the dynamic reciprocal interactions between the two phases within a non-homogeneous debris flow.

2. Experimental Program

2.1 Experimental site and devices

The experimental site is located in the Jiangjia gully where about 28 natural debris-flow events occur annually (Cui et al., 2005), with each occurrence containing tens to hundreds of surges (Liu et al. 2009). Seasonally-centered rainfalls (i.e. with the mean annual rainfall

ranging from 400 to 1000 mm, 85% of which concentrates between May and October), easily-weathered materials (i.e. slate, dolomite and phyllite) and lack of the vegetation covers jointly contribute to the frequent recurrence of debris flows within the region. Thus it makes an ideal field site to carry out the experimentally-generated debris flows to test the proposed two-phase flow model, before extending its applications to the natural debris flows. In our experiment, a small upstream gully area was selected and the location map is shown in Figure 1 (Note: our experimental flows were triggered by artificially releasing a volume of water).

The perennial flow conditions and gully dimensions provided suitable conditions for the generation of non-homogeneous debris flows in terms of providing the necessary upstream water supply (i.e. replacing the role of intensive rainfalls) and four effective zones of the debris flow motion including its initiation, transportation, transition and deposition from the upper to lower stream. More importantly, the steep slope of the gully (i.e. Site B in Figure 1) and the abundance of loose materials (both fine and coarse particles) on both sides of the bank contributed to the generation of debris flow in non-homogeneity, and the gully bed appeared to be non-erodible as it was composed of the large bedrocks. Similar experimental debris flows were also observed in both the transition and deposition zones during the field surveys conducted in 2008 and 2009, respectively. Field observations of these naturally-generated debris flows were made by Kang et al. (2006) at the Dongchuan Debris Flow Research Station, which is also shown in Figure 1 (i.e. Site A).

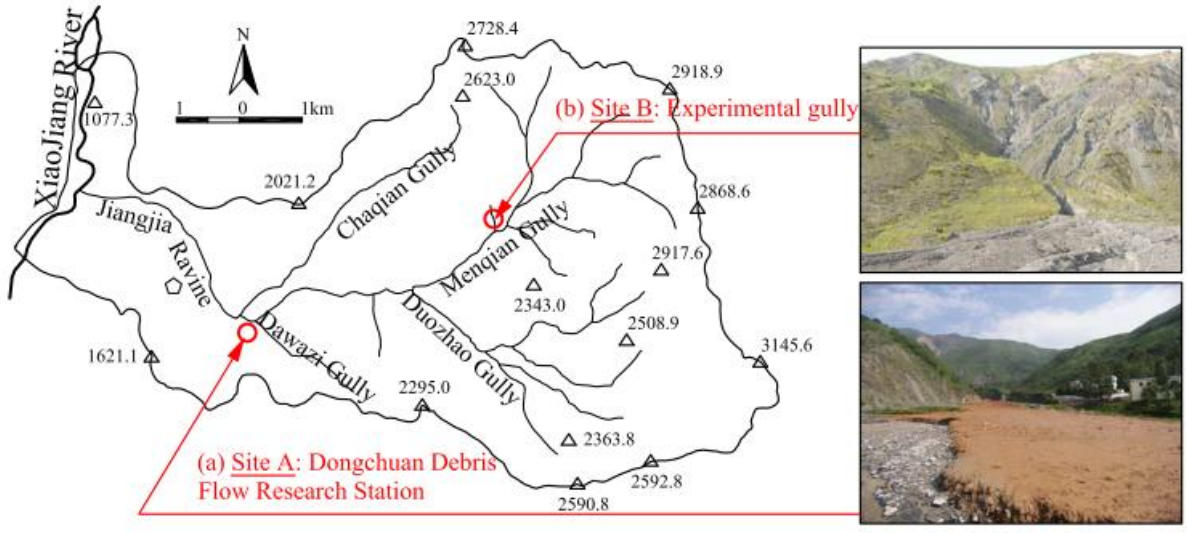

Figure 1: Field site of (a) natural; and (b) experimental non-homogeneous debris flows

In order to generate the detailed profile of the gully as shown in Figure 2(a), an electronic theodolite and a scale were employed to measure the horizontal distance and elevation difference between two successive points within the thalweg of the gully, and this was carried out from the downstream to upstream. A video camera was installed on the right bank of the channel (viewed from the upstream to downstream) with a tripod to record the debris-flow process at the observation site [see Figures 2(a) and 2(c)]. The debris flows were manually sampled when the flow passed through the observation section, with a bucket being vertically inserted into the flow body (near the rear of the front surge) to obtain the samples for further analysis. It should be noted that the debris-flow velocity was derived from the time and mobilization of debris flows throughout a given distance from the video tapes (i.e. the colored plastic beads that "floated" on the debris-flow surface were used as the tracers to derive the average flow velocity), while its flow depth and width were obtained by measuring the imprints of a past debris flow event on both sides of the observation post (i.e. mudlines) by a scale. The gully generally exhibited a trapezoidal cross-section on the observation site, thereby facilitating the measurement of flow depth and width. These measurements (i.e. samples collection, flow depth and width) were restricted to the same cross section for each debris flow test. Besides, other supplementary equipments provided by the Dongchuan Debris Flow Research Station (e.g. electronic shaker, rheological systems, etc.) were used to derive other post-experimental data (e.g. grain size distribution).

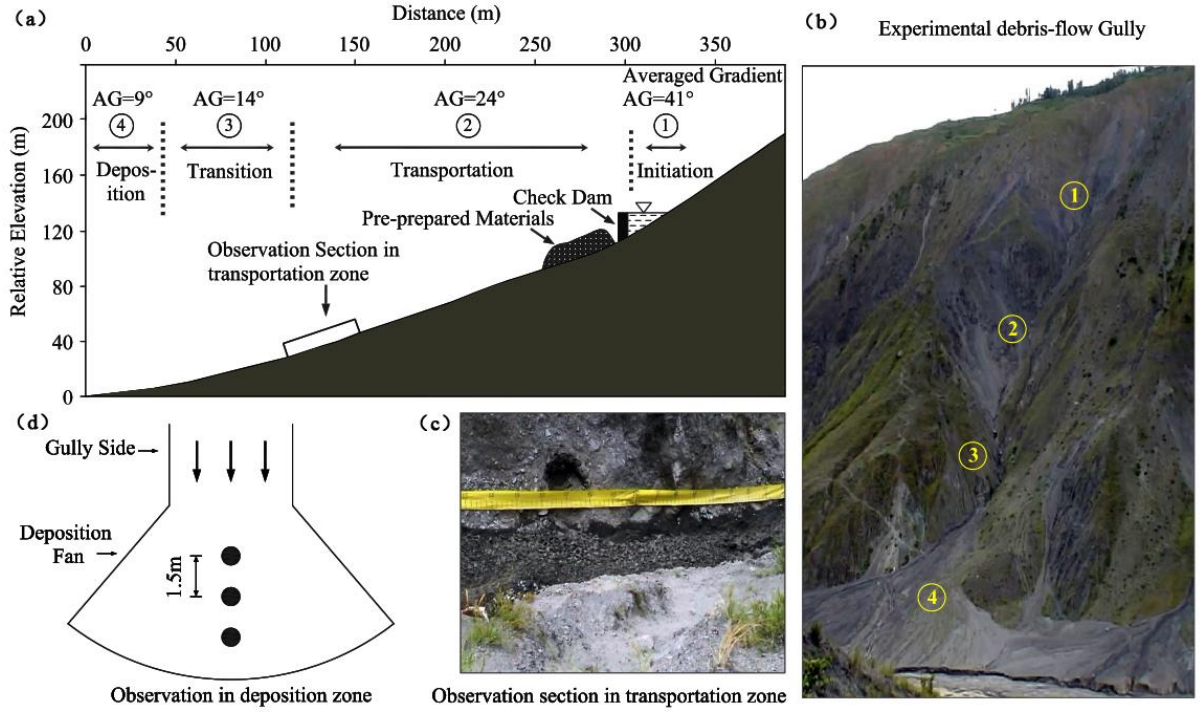

Figure 2: Schematic view [(a): profile and sub-divided reaches of the gully; (b): front view; (c): side view of the observation section; and (d): plan view of the schematic deposition zone] of debris-flow transport route and deposit fan

2.2 Experimental conditions

The longitudinal profile of the gully is shown in Figure 2(a). It is seen that the averaged gradient of the gully bed consistently decreases from the upstream to downstream end [S_0 = 0.869 (41°) to S_0 = 0.158 (9°)], and the gully is characterized by four distinct reaches (i.e. initiation, transportation, transition and deposition), which is favorable for generating and investigating the debris flows. Specifically, the upstream end within the gully is shown to be a convergent area for the erodible materials and flows, and the averaged gully width is below ~1.0 m. In the transportation reach with S_0 = 0.445 (24°), a large volume of loose particles located on both sides of the gully provide additional material supplies for the bypassing debris flows. The end of this reach is relatively straight and easily accessible, thus an observation zone is placed. The transition reach is also easily distinguishable due to its larger value of the averaged width (i.e. 2.0 m) and the reduced gradient [S_0 = 0.249 (14°)]. The downstream end demonstrates a much lower gradient [S_0 = 0.158 (9°)] and thus provides a

wide topographic area for the debris-flow deposition.

The materials for forming the debris flows in the gully were sampled and the details of grain size composition are presented in Figure 3. It should be noted herein that the source materials were completely dried and manually sampled before being saturated and entrained by the running flows. Also, these source materials were only collected at the beginning of the experiment, and the sampling processes were not repeated prior to each test. The material has a wide sediment size ranges from the clay to the gravel, and the content of particles with $d <$ 2.0 mm varies between 28% and 35%, which is ideal for producing the non-homogeneous debris flows. Our experiments were carried out in the rainy seasons (i.e. August and September) when the gully has an averaged base flow (i.e. Q = 0.02 m^3/s). For safety purpose, however, the experiments were usually undertaken in the days without the rainfall, and thus the base flow is expected to experience some slight variations.

The present study includes the data of 31 debris flows generated in the experimental gully, with 25 tests for the transportation zone and 6 tests for the deposition zone. Further 9 datasets of the natural field debris flows (Kang et al., 2006) measured in the transportation zone at Dongchuan Debris Flow Research Station (i.e. Site A in Figure 1) are also included. The parameters characterising all the debris flows in the current study are presented in Table 1. It is shown that the values of the debris-flow density γ_m range 1.80 ~ 2.32 t/m^3, which represents the typical debris flows observed in the Jiangjia gully. Additionally, the values of other parameters (such as the flow depth, width etc.) in natural debris flows are relatively higher than those in the experimental counterpart, which will be discussed below. Note that the measurement for the debris flows in the deposition zone is limited to the bulk density γ_m.

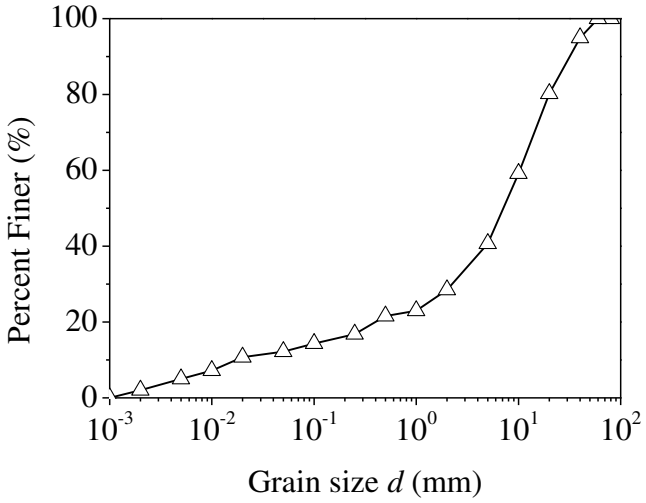

Figure 3: Grain size distributions of loose material forming debris flows at the upstream gully

Table 1: Hydraulic conditions measured for all tested debris flows

Debris flow	Run #	Bulk Density γ_m (t/m^3)	Flow Depth h (m)	Flow Width W (m)	Hydraulic Radius R (m)	Measured Velocity U_0 (m/s)	Flow Rate q (m^2/s)	Froude Number Fr
Natural (Site A in Figure 1)[1]	N1	2.190	1.00	27	0.93	7.63	7.63	2.44
	N2	2.090	0.90	15	0.80	7.63	6.87	2.57
	N3	2.150	0.70	22	0.66	5.87	4.11	2.24
	N4	2.150	1.27	23	1.14	5.50	6.99	1.56
	N5	2.164	1.10	26	1.01	10.0	11.0	3.04
	N6	2.186	0.55	-	0.55	6.63	3.64	2.85
	N7	2.074	0.90	40	0.86	7.63	6.87	2.57
	N8	2.206	0.95	20	0.87	7.31	6.94	2.39
	N9	2.251	0.80	30	0.76	7.36	5.89	2.63

Experimental (Site B in Figure 1)[1] (2008)	E1	2.119	0.33	0.86	0.18	3.32	1.10	1.85
	E2	2.117	0.39	1.02	0.20	4.00	1.56	2.05
	E3	2.106	0.29	0.98	0.18	2.88	0.84	1.71
	E4	2.098	0.32	1.36	0.19	3.42	1.09	1.92
	E5	2.031	0.40	0.96	0.19	2.76	1.10	1.39
	E6	2.123	0.60	1.35	0.22	3.72	2.23	1.53
	E7	2.186	0.19	0.70	0.15	2.72	0.52	1.99
	E8	2.127	0.60	1.13	0.23	2.98	1.79	1.23
	E9	2.205	0.60	1.08	0.24	3.88	2.33	1.60
	E10	1.989	0.35	0.78	0.17	2.49	0.87	1.34
	E11	2.181	0.43	0.77	0.20	4.05	1.74	1.97
	E12	2.191	0.34	0.89	0.19	2.97	1.01	1.63
	E13	2.217	0.50	1.05	0.22	4.04	2.02	1.82
	E14	2.226	0.48	1.05	0.22	4.46	2.14	2.06
	E15	2.265	0.30	0.87	0.18	3.07	0.92	1.79
	E16	2.198	0.60	1.25	0.24	4.05	2.43	1.67
	E17	2.244	0.36	0.78	0.19	3.76	1.35	2.00
	E18	2.219	0.47	0.79	0.21	3.44	1.62	1.60
	E19	1.861	0.38	0.83	0.16	3.20	1.22	1.66
	E20	2.147	0.44	0.81	0.20	4.48	1.97	2.16
	E21	2.246	0.45	0.64	0.20	3.41	1.53	1.62
	E22	2.219	0.18	0.58	0.14	2.64	0.48	1.99
	E23	2.193	0.22	0.64	0.15	3.34	0.73	2.27
	E24	1.993	0.25	0.69	0.15	3.00	0.75	1.92
	E25	2.219	0.24	0.69	0.16	3.47	0.83	2.26
Experimental (Site B in Figure 1)[2] (2009)	E26	1.800	-	-	-	-	-	-
	E27	2.230	-	-	-	-	-	-
	E28	1.870	-	-	-	-	-	-
	E29	1.980	-	-	-	-	-	-
	E30	2.320	-	-	-	-	-	-
	E31	2.080	-	-	-	-	-	-

[1] transportation zone; [2] deposition zone. Note: U_0 = measured bulk velocity of debris-flow body (near the rear of the front surge); q (=Q/W) is the unit-width flow rate measured at the observational cross section; $F_r = U_0 / \sqrt{gh}$ is applicable to the gully-type debris flows.

2.3 Experimental setup and procedure

A schematic representation of the experimental set-up of the gully is shown in previous Figure 2. Before each run, a simple check dam with a gate was temporarily constructed at the upstream end of the gully to impound a natural stream flow. 3 - 5 tons of loose, well-sorted dry materials, collected from both sides of the gully, were randomly placed upstream of the dam (Figure 2). When the stream flow just began to overtop the check dam, the gate was opened and the graded sediments were entrained by the released water flow, and the moving materials and flow mixed quickly and migrated rapidly over the steep upstream reach. After the flow and sediment were thoroughly mixed, the generated debris flow propagated down the gully towards the transportation zone, which includes an observational reach to collect the samples of the debris flows and measure the flow depth. In addition, a video camera was set up on the right side of the observational reach to record the debris flow motion, allowing their velocities to be obtained with reference to a buoy and distance indicator which is marked on the left side of the gully. The particle size distribution of one debris-flow sample was measured through the rheology test (for the fine grain size $d \leq 2.0$ mm) and the sieving analysis (for the coarse grain size $d \geq 2.0$ mm). The rheology test has been commonly adopted to establish the relationship between the shear stress/viscosity and the shear rate and further describe the behaviour of debris flows based on the consolidated rheological theories such as the Newtonian fluids, Bingham plastic fluids, etc. (Major and Pierson, 1992; Santolo et al., 2010). Meanwhile, the bulk density γ_m was determined by the iso-volume method (Chen et al., 2003) using $\gamma_m = M/V$, where M is the mass of debris-flow sample and V is the volume of clear water equivalent to the debris-flow sample. Furthermore, in order to analyze the vertical variation of grain size distributions, the sediment samples were obtained from the upper to lower layers of the deposit zone at three 1.5 m - spaced sampling points along the centre of the depositional fan (as shown in Figure 2). It should be mentioned that the data for the natural debris flows were collected in a manner similar to the experimental counterparts (Kang et al., 2006), and the only difference lies in that the natural ones have a wider and shallower channel (see Table 1).

Undoubtedly, there are some uncertainties associated with the field observations in the

current study: (i) the density of a debris flow should be predominantly governed by the relative proportions of the liquid flow and the solid material that it contains. However, it is impossible to identify the exact quantity of those loose materials in the initiation zone (Figure 2); and (ii) the observation of the debris flows was only made at the specific locations of the gully, so it is unknown whether the new materials have been incorporated or not as the debris flows passed through the transportation zone. Consequently, it is uncertain of the variability in the composition of a debris flow along its running course within the present study. Of course, these uncertainties should be reasonably accepted given that the field conditions are always difficult to be well-controlled.

2.4 Experimental data analysis

The experimental and natural debris flow measurements conducted in the transportation zone indicated a wide grain size distribution (d = 1 μm ~ 100 mm) as shown in Figure 4. However, the median grain size d_{50} is shown to be finer, and the measured standard deviations σ_g to be an order of magnitude higher, for the natural debris flows as compared with the experimental ones. This is mainly due to the higher concentration of the fine particles (d < 1.0 mm) existing in the natural debris flows.

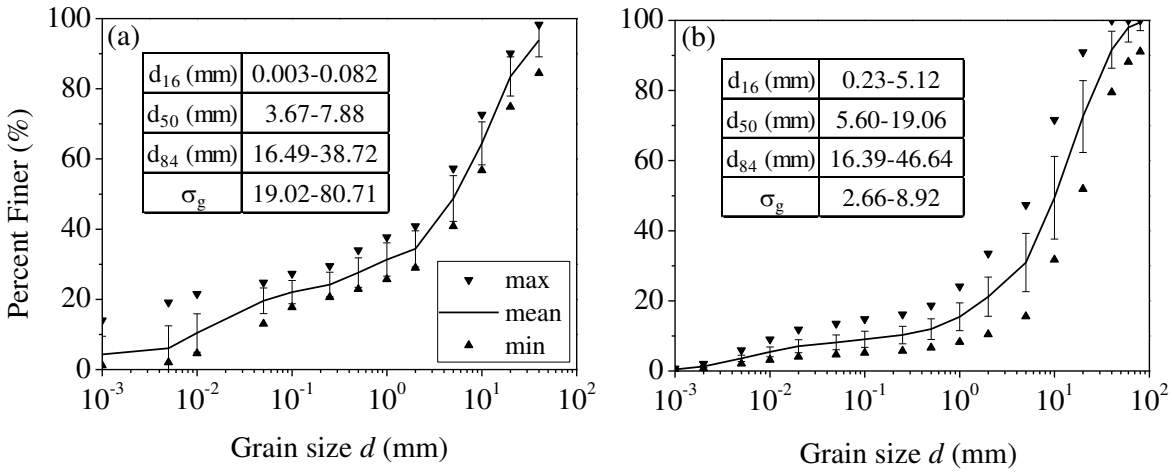

Figure 4: Grain size distributions of debris flow in the transportation zone: (a) natural debris flow; and (b) experimental debris flow

All the experimental and natural debris flows provided in Table 1 also exhibit discrepancies

with respect to their hydraulic conditions. Kinematic similarity between the two can be described by the Froude number $F_r = U_0 / \sqrt{gh}$, which represents the ratio of the inertial to gravitational forces of the flowing mass. From Table 1, it is shown that F_r values range from 1.56 ~ 3.04 and 1.23 ~ 2.26, respectively, for the natural and experimental debris flows and thus they can be considered kinematically similar (i.e. supercritical flow). The main difference between the two flows lies in the geometric similarity, in which a combination of shallower flow depth and higher velocity gives rise to the larger F_r values in the natural debris flows. Nevertheless, what is common to both the experimental and natural debris flows is that most of them were found to have high bulk densities with γ_m > ~ 2.0 t/m^3.

3. Two-Phase Velocity of Non-Homogeneous Debris Flow

On the basis of the Darcy-Weisbach equation (Chow, 1959), the minimum energy equilibrium and some theories related to the debris flow, combined with our previous studies (Shu et al., 2010), a theoretical model for the liquid and solid phases transported within the non-homogeneous debris flows will be briefly provided in the following sections. For more details the reader may refer to Shu et al. (2007).

3.1 Determination of critical diameter d_0

The energy dissipated by the two phases in a non-homogeneous debris flow can be conveniently described by the energy gradient of the liquid phase J_l and the solid phase J_s. The total energy gradient J therefore equates to the summation of the contributions from both phases, i.e.

$$J = J_l + J_s \tag{1}$$

In order to attain the equilibrium between the scour and deposition, the transportation of non-homogeneous debris flows must be considered as a dynamic process involving the exchange of coarse particles from the solid phase and fine particles from the liquid phase, with their mobilizations and rheological characteristics being adjusted to the spatial and

temporal variations of the flow and sediment conditions (Iverson et al., 1997c). Accordingly, the related sedimentary and hydraulic factors should be adjusted towards the minimum dissipated energy, for which the energy gradient J_l of the liquid phase can be derived from a modified form of the Manning's formula (Fei and Shu, 2004) as

$$J_l = J \times \frac{\gamma_f}{\gamma_m} = \frac{f}{8} \times \frac{U^2}{gR} \times \frac{\gamma_f}{\gamma_m} \tag{2a}$$

$$J_l = \frac{1}{gR}\left[27.8\omega_0 C_{vf}^{2/3}\left(\frac{4R}{d_0}\right)^{\frac{1}{9}}\right]^2 \frac{\gamma_f}{\gamma_m} \tag{2b}$$

where R is the hydraulic radius; γ_f and γ_m are the bulk densities of the liquid phase and debris flow mixture, respectively; ω_0 is the settling velocity corresponding to the critical grain size d_0 (Shu et al., 2008); and C_{vf} is the volumetric concentration of the liquid phase. The corresponding energy gradient of the solid phase J_s can be established based on Bagnold's (1954) theory as

$$J_s = C_{vc}\left(\frac{\gamma_s - \gamma_f}{\gamma_m}\right)\tan\alpha \tag{3}$$

where C_{vc} is the volumetric concentration of the solid phase, and $C_{vc} = X \cdot C_v$, where C_v is the volumetric concentration of the debris-flow mixture and X is the assumed weight proportion of the solid phase; and $\tan\alpha$ is a macro frictional factor arising from the interactions between the coarse particles. As shown from Eqs. (2) and (3), the energy gradient of the liquid and solid phases in a non-homogeneous debris flow is closely related to the assumed critical diameter d_0 [note: in Eq. (3), J_s is proportional to the solid phase concentration C_{vc}, which is also in-turn determined by the solid-phase weight proportion X, and hence ultimately related to d_0 as well]. By combining Eqs. (1), (2) and (3), the total energy gradient towards the minimum loss is given as

$$J = J_l + J_s = \frac{1}{gR}\left[27.8\omega_0 C_{vf}^{2/3}\left(\frac{4R}{d_0}\right)^{\frac{1}{9}}\right]^2 \frac{\gamma_f}{\gamma_m} + XC_v\left(\frac{\gamma_s - \gamma_f}{\gamma_m}\right)\tan\alpha \rightarrow J_{\min} \tag{4}$$

Previous results by Shu et al. (2008) demonstrated that for all the non-homogeneous debris flows, as the critical diameter d_0 increases, J_l increases but J_s decreases monotonically, while

the resulting total energy gradient $J = J_l + J_s$ increases after an initial decrease (see Figure 5). Hence, J should attain a minimum value J_{min} under a constant hydraulic radius, which corresponds to the critical diameter d_0 separating the solid and liquid phases, as indicated in Figure 5.

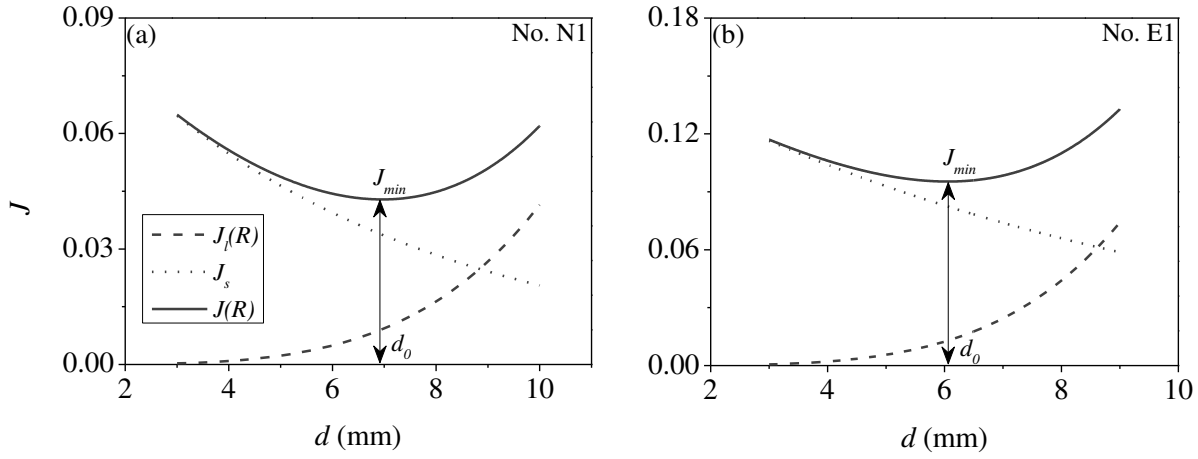

Figure 5: Schematic relationship between d_0 and J_s, J_l and J_{min} for (a) natural debris flow N1; and (b) experimental debris flow E1

3.2 Expressions of liquid-and-solid phase velocity

According to the above determination of the critical diameter d_0, the liquid and solid phases in a non-homogeneous debris flow can be quantitatively separated. Detailed information on the derivation of velocities for the liquid and solid phases within non-homogeneous debris flows are given by Shu et al. (2010). Herein, the theoretical equations for the liquid and solid phases can be expressed as

$$U_l = 27.8\sqrt{\frac{8}{f_m}}\omega_0 \cdot C_{vf}^{2/3}\left(\frac{4R}{d_0}\right)^{\frac{1}{9}} \tag{5}$$

and

$$U_s = U_l\left(\frac{C_{vm}}{1-C_{vc}} - C_{vc}\right) \tag{6}$$

where f_m is the Darcy-Weisbach frictional factor of the debris-flow mixture and specified by Fei and Shu (2004); C_{vm} is the limited concentration defined by Fei and Shu (2004), which

arises from the wide range of particle sizes contained within the non-homogeneous debris flows and results in the interstitial filling of fine particles (in the liquid phase) with the coarse grains (in the solid phase). With further analysis using the two-phase velocity assumptions, an averaged velocity of the debris flow, U_c can be expressed in the following form:

$$U_c = \frac{U_l C_{vf} + U_s C_{vc}}{C_{vf} + C_{vc}} \tag{7}$$

3.3 Computational procedure of two-phase model

In order to illustrate the model application, a step-wise procedure is recommended for deriving the key information such as the critical grain diameter and the velocities of liquid and solid phases. The input data to the two-phase model mainly include the hydraulic radius R, bulk density γ_m and grain size distribution of the collected samples (i.e. Table 1 and Figure 4), while the remaining parameters can then be calculated, where the important outputs (e.g., J_{min}, d_0, U_l, U_s and U_c) can be determined through the trial-and-error method presented in Figure 6.

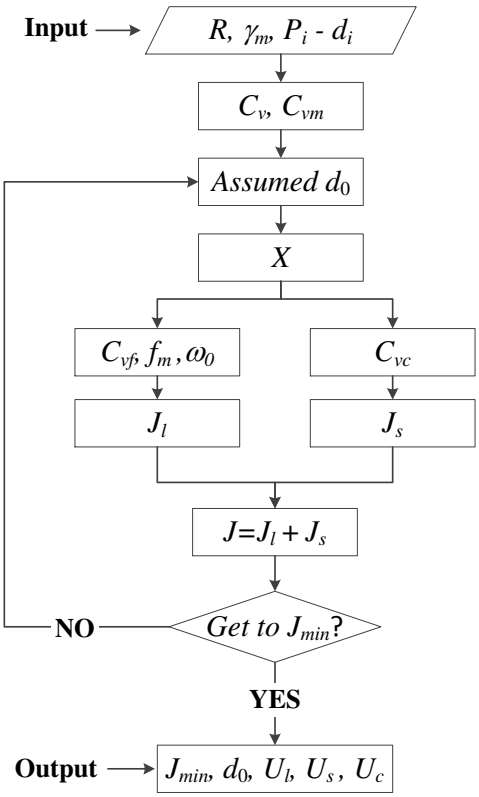

Figure 6: Computational procedure chart of the model application (where P_i is the weight proportion corresponding to the specific grain size d_i and available from the curve of grain size distribution)

4. Results and Analysis

4.1 Critical diameter d_0 of debris flows

The critical diameters d_0 of 34 non-homogeneous debris flow runs were found by using the method outlined in Section 3.1 and Figure 6, to range 5.6 mm – 7.0 mm and 4.7 mm – 6.3 mm, respectively, for the natural and experimental debris flows (see Figures 7a-1,b-1). This has been found to agree well with the size of suspended particles within the debris flows observed in Jiangjia gully (Wu et al., 1993), as well as from other field investigations (e.g., Shu et al., 2008; Yang et al., 2014).

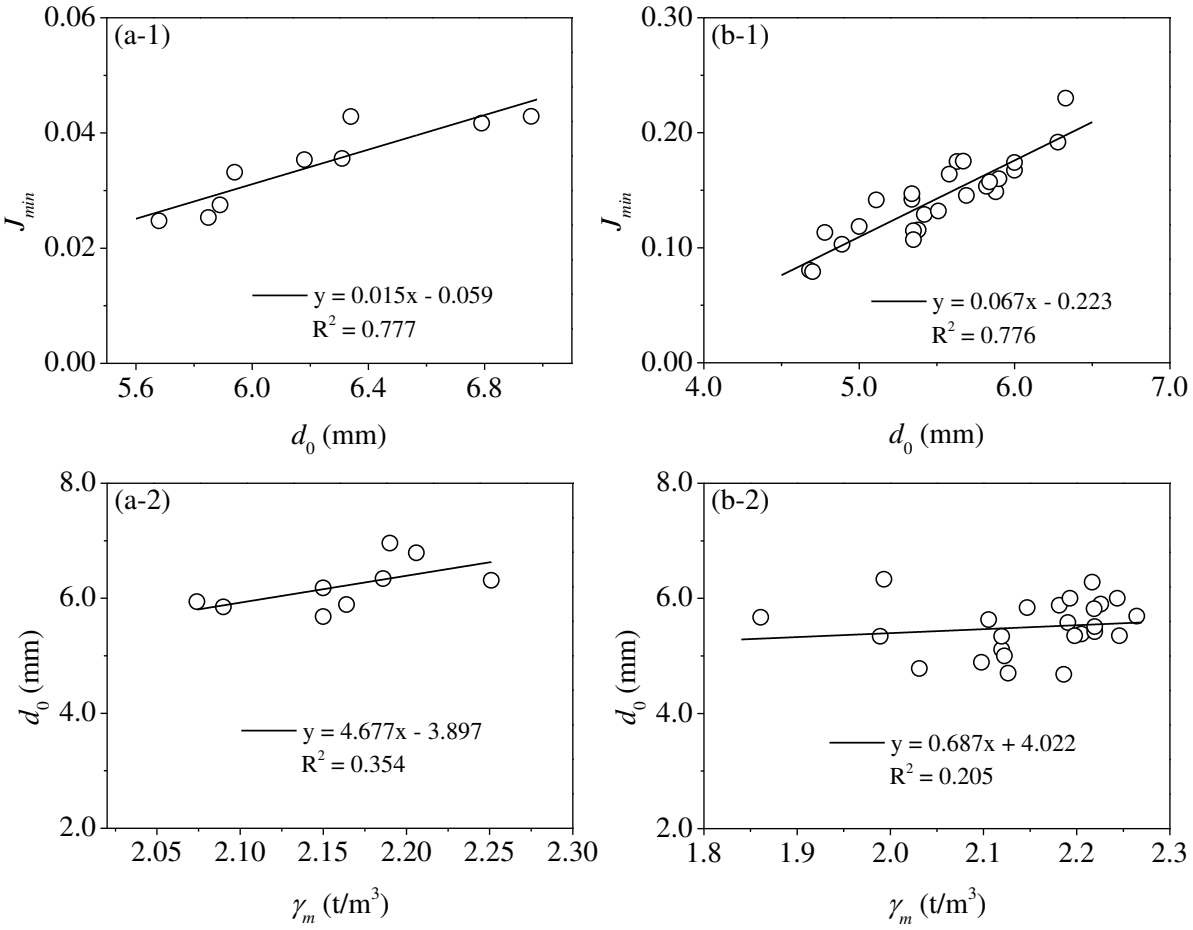

Figure 7: The relationships between γ_m and calculated J_{min}, d_0 for (a) natural debris flow; and (b) experimental debris flow

It is demonstrated in Figure 7 that the calibrated critical diameter d_0 increases with the minimum dissipated energy J_{min} and the bulk density of the debris flows γ_m (see Figures 7a-2,b-2). This seems to be reasonable, since an increase of the bulk density γ_m indicates a higher proportion of the sediment contents existing in the debris flow, as well as a higher proportion of the coarser particles.

Furthermore, as the J_{min} increases with the increase of d_0 (Figures 7a-1; 7b-1), and the d_0 increases with the increase of debris-flow density (Figures 7a-2; 7b-2), the minimum dissipated energy J_{min} would also be reasonably expected to increase for the debris flows with higher bulk densities γ_m, and accordingly, with higher critical diameters d_0. The present results are also consistent with the previous study from Shu et al. (2008) and recent research

from Yang et al. (2014).

4.2 Relative velocities of liquid and solid phases

By using Eqs. (5) and (6), with the obtained critical diameter d_0, the velocities of the liquid and solid phases of the 34 natural and experimental debris flows were calculated. The liquid velocity U_l and solid velocity U_s were found to range 2.56 ~ 4.51 m/s and 2.04 ~ 4.48 m/s, respectively, for the experimental debris flows; and between 6.02 ~ 10.84 m/s and 5.04 ~ 9.69 m/s, respectively, for the natural debris flows. Figure 8 shows the magnitude of U_l and U_s values for the different debris-flow bulk densities γ_m, with $U_l > U_s$ being shown for the majority of the debris flows (Figures 8a-1, b-1). This corresponds to the conditions under which the solid particles are entrained by the liquid flows. At the lowest bulk densities γ_m, the debris flows demonstrate the largest difference between the liquid and solid phase velocities ($U_l > U_s$), although this difference is shown to reduce with the increasing γ_m. The reason is attributed to the increase of the solid-phase particles, which leads to an increasingly important role of the solid phase in the transportation dynamics of the non-homogeneous debris flow. Indeed, for both the natural and experimental debris flows with the highest bulk densities (Figures 8a-2, b-2), the calculated velocity of the solid phase is shown to exceed that of the liquid phase (i.e. $U_s > U_l$). Within the current study, the composite velocity of the debris flows was measured at one location and a specific time. It should be noted, however, that due to the continual variations in both the sediment composition and gully geometry, this composite velocity (and hence the corresponding two-phase velocities) would be expected to vary spatially and temporally at different locations along the flow path.

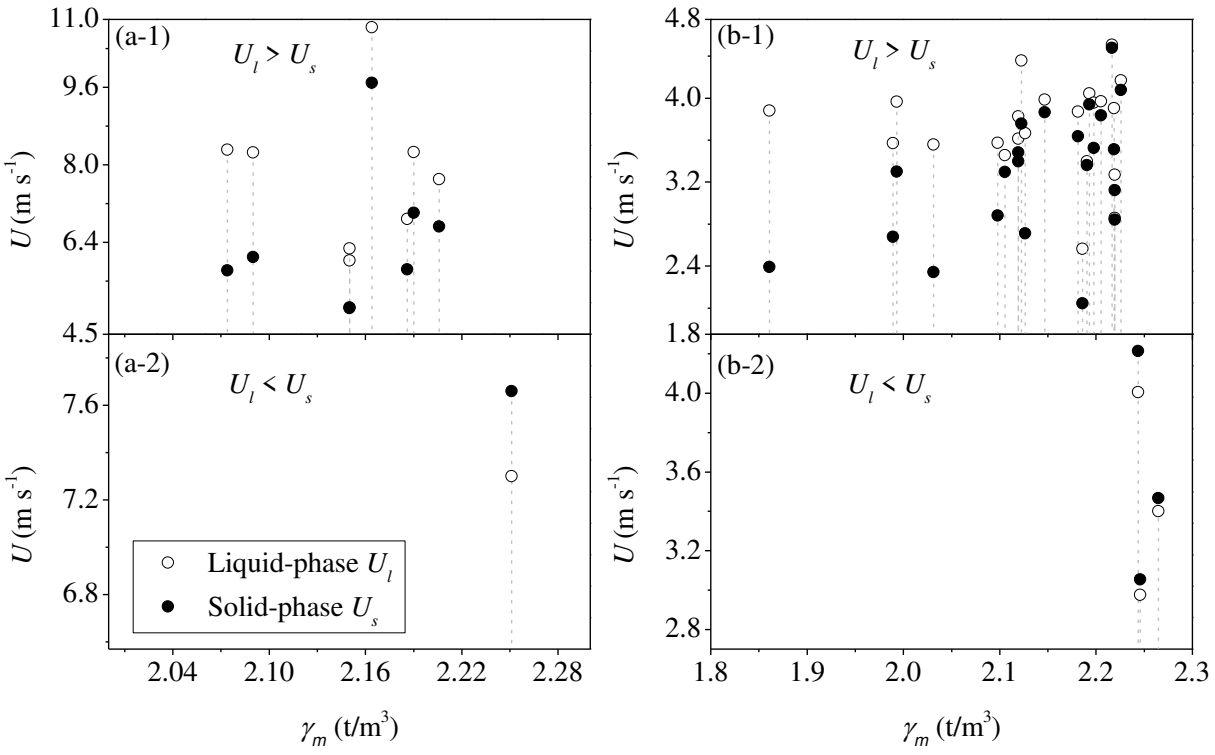

Figure 8: Predictive velocity of the liquid and solid phase within (a) natural debris flow; and (b) experimental debris flow by using Eqs. (5) and (6)

The velocity ratio between the liquid and solid phases can be defined as $\eta = U_l/U_s$, which reflects the relative velocity between the two phases. The velocity ratio η is dimensionless and plotted against the specific gravity λ ($\lambda = \gamma_m/\gamma$, where γ is the water density) in Figure 9. It is shown that a critical specific gravity $\lambda_0 = 2.237$ and $\lambda_0 = 2.247$ can be determined for the experimental and natural debris flows, respectively, where the velocity difference between the two phases diminishes (i.e. $\eta = 1$). When the specific gravity λ is significantly lower or higher than the critical values λ_0, the influence of any single phase (i.e. liquid or solid phase, respectively) becomes more dominant on the overall dynamic behaviours of the debris flow, and the relative differences between U_l and U_s increase, namely the liquid phase dominates the motion of the mixture when η is considerably larger than 1.0 (e.g. hyper-concentrated flow as an extreme case), and the solid phase dominates the motion when η is significantly lower than 1.0. It is clear from the results that the two-phase velocities of both the experimental and natural debris flows follow the same trend. It should also be highly noted that the critical specific gravity (λ_0) derived for the experimental and natural debris flows is

very close, which is quite encouraging if considering the different conditions (e.g., flow depth, width, etc.) measured in both cases. This suggests the present model can be applied to a wide range of debris flow studies in the practical field.

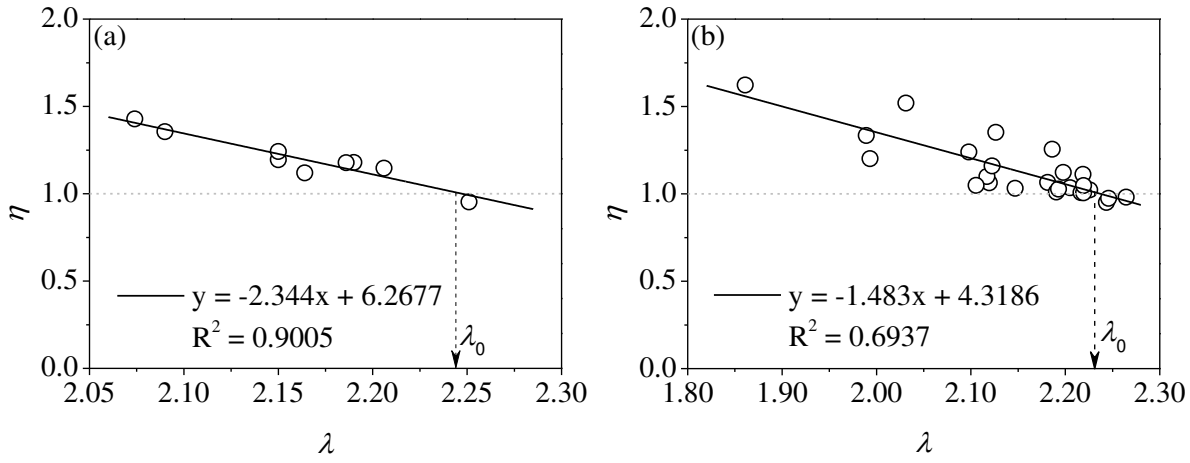

Figure 9: Ratio of liquid-phase U_l to solid-phase U_s for (a) natural debris flow; and (b) experimental debris flow

4.3 Deposition patterns of debris flow

The median grain diameters from the upper (d_{u50}) and lower (d_{l50}) layers of the debris deposits obtained from six experimental tests in the deposition zone (in Table 1), are shown in Figure 10, the upper and lower layer corresponds to 0 – 0.5H and 0.5 – 1.0H (H is the thickness of debris-flow deposits), respectively. These are averaged over the three sampling locations (as seen in Figure 2) to realistically represent the spatial grain distribution patterns and eliminate the data fluctuations from single point of measurement. These grain size measurements provide basic information on the variations of the vertical depositional patterns, indicating that for the debris flows with the lower bulk densities (i.e. γ_m < ~2.10 t/m^3), the median particle size in the upper layer remains virtually constant (d_{u50} = 1.85 ~ 2.23 mm), whilst reducing slightly in the lower layer (d_{l50} = 17.63 → 15.68 mm) as γ_m reduces from 2.10 → 1.80 t/m^3. In contrast, for the debris flows with the higher bulk densities (i.e. γ_m > 2.10 t/m^3), the median grain size in the upper layer increases significantly (d_{u50} = 1.85 → 21.97 mm) as γ_m = 2.10 → 2.30 t/m^3, while in the lower layer the corresponding median grain size reduces (d_{l50} = 17.63 → 11.71 mm) over the same range. The upper and lower layers have the

same median grain size (i.e. $d_{u50} \approx d_{l50}$ = 12.60 ~ 12.80 mm) for the debris flows with bulk density γ_m = 2.23 t/m^3. As a result, the deposits of a non-homogeneous debris flow can be given in the following classifications: (i) *"normal"* graded deposits (N) when $d_{l50} > d_{u50}$ (i.e. for $\gamma_m <$ 2.23 t/m^3); (ii) *"mixed"* graded deposits (M) when $d_{l50} \approx d_{u50}$ (i.e. for $\gamma_m \approx$ 2.23 t/m^3); and (iii) *"inverse"* graded deposits when $d_{l50} < d_{u50}$ (when $\gamma_m >$ 2.23 t/m^3). Also, the averaged value (d_{ave50}) between the upper (d_{u50}) and lower (d_{l50}) layers are also presented in Figure 10. It is shown that d_{ave50} appears to increase with the bulk density γ_m, particularly when it exceeds 2.10 t/m^3. This is consistent with the relationship between d_0 and bulk density γ_m given in Figure 7, which further implies a continuous increase of the coarse particles as the bulk density γ_m increases within the non-homogeneous debris flows.

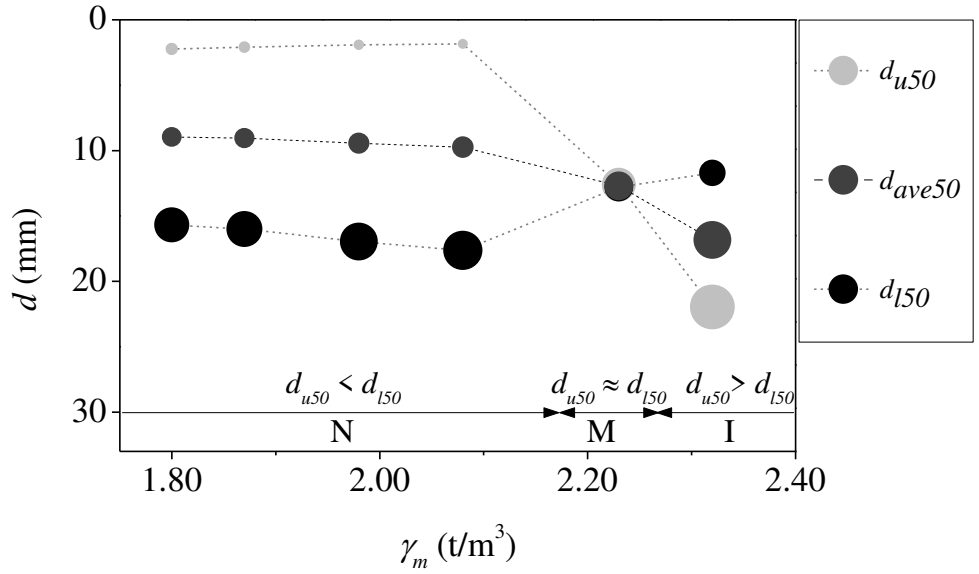

Figure 10: Median grain size in the upper (d_{u50}) and lower (d_{l50}) layers of debris flow deposits, and their average value (d_{ave50}), as function of the bulk density γ_m (N - normal grading; M - mixed grading; I - inverse grading)

It is interesting to note that these grading patterns observed in the deposition zone appear to be similar to the findings from the other 25 experiments conducted in the transportation zone. Especially, the critical bulk density $\gamma_m \approx$ 2.23 t/m^3 used for separating the two-phase velocities is also applicable to the delineation of deposit grading patterns. That is to say, the debris flows with relative phase velocity ratios $\eta > 1$ and $\eta < 1$, correspond to the normal and

inverse grading patterns in the deposition zone, respectively. This suggests that the depositional grading pattern of a non-homogeneous debris flow corresponds well to the relative motion predicted for the liquid and solid phases within the transportation zone in the same gully if considering their correlations with the debris-flow bulk density γ_m.

5. Discussions

5.1 Validations of predicted debris flow velocity

Further analysis of the data revealed that the observed velocity U_0 of the natural and experimental debris flows lies between the liquid and solid phase velocities of U_l and U_s. This was found by comparing the differences between the observed and calculated two-phase velocities based on the velocity ratio $\varphi_l = U_l/U_0$ and $\varphi_s = U_s/U_0$ versus the specific gravity λ of the debris flows. Figure 11(a) and (b) shows the results for the natural and experimental debris flows, respectively. It is shown that the observed debris flow velocities are generally lower than the calculated liquid-phase velocities (i.e. $\varphi_l > 1.0$) and higher than the calculated solid-phase velocities (i.e. $\varphi_s < 1.0$) for both debris flows below the critical bulk density. By contrast, the opposite trend (i.e. $\varphi_l < 1.0$ and $\varphi_s > 1.0$) occurs when the bulk densities of the experimental and natural debris flows exceed their critical values.

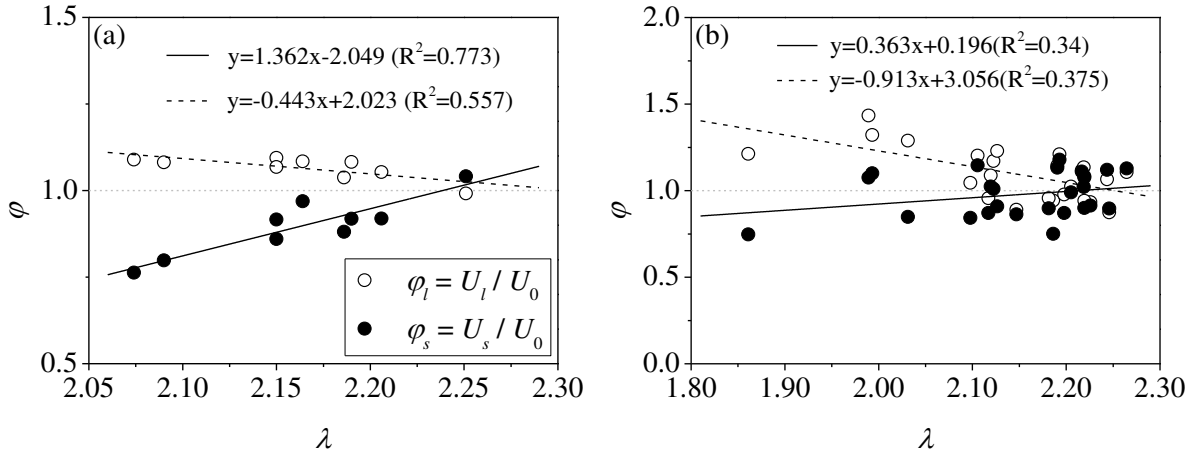

Figure 11: Ratio of the calculated two-phase velocities (U_l, U_s) to the observed velocity (U_0) for (a) natural debris flow; and (b) experimental debris flow

Based on the liquid and solid phase velocity for each debris flow, a composite averaged velocity U_c can be calculated from Eq. (7). The proposed two-phase debris flow model can therefore be validated by comparing the calculated U_c with the observed U_0 for both the natural and experimental debris flows (as shown in Figure 12). It is shown that the model is satisfactory in predicting the composite velocities as well over the range of test conditions. This good agreement is achieved partially owing to a small dataset used.

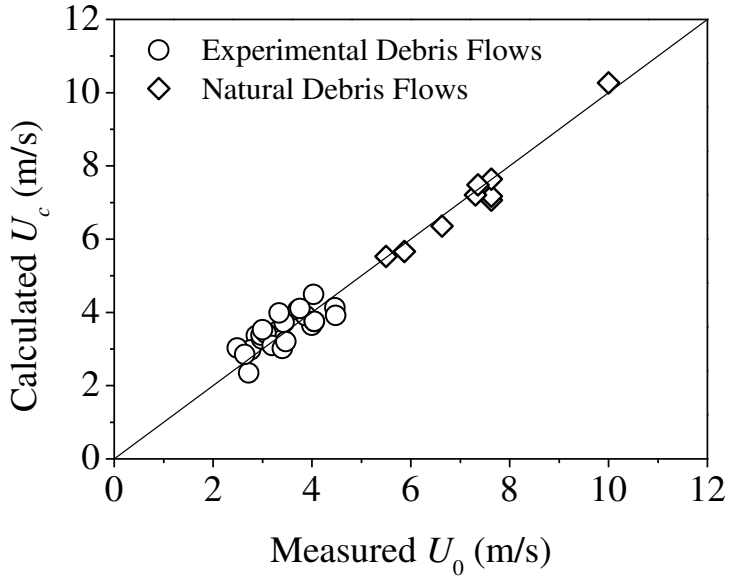

Figure 12: Measured U_0 versus calculated U_c

5.2 Two-phase motion and vertical grading pattern

The datasets from the experimental and natural debris flows indicate that the differences between the phase velocities U_l and U_s [determined from Eqs. (5) and (6), respectively, shown in Figs. 8 and 9] matched quite well with the different deposition grading patterns of the observed non-homogeneous debris flows (see Figure 10). Now consider three possible flow scenarios (see Figure 9): (i) $U_l > U_s$ – typical for the common muddy and full-turbulent debris flows that can be simulated by a two-phase model. In such cases, fine particles in the liquid phase could be regarded as suspended load and coarse grains in the solid phase as bed load; (ii) $U_l \approx U_s$ – the respective velocity of each phase is ideally equivalent. This type of the mixed debris flow could be adequately simulated by a single-phase model [i.e. one momentum equation, as in Fraccarollo and Papa (2000)]; and (iii) $U_l < U_s$ – which only

occurs for the debris flows with extremely high bulk density γ_m. Only 4 of the 34 non-homogeneous debris flows considered in the present study fall into this category.

Although the data set collected from the debris flow deposition zone is limited to 6 runs, they can be viewed as good representations of the field case. This is due to that the bulk density typically spans a wide range (i.e. 1.80 – 2.32 t/m^3), which is similar to the data set collected in the transportation zone (see Table 1). As mentioned before, the dynamic interactions between the different particle phases are complex and can result in the vertical size gradation of the debris flow deposits. For scenario (i), the debris flows with a higher liquid-phase velocity (i.e. $U_l > U_s$, which is prevalent in most debris flows with lower bulk densities γ_m) could be described by a dominant suspended transport load model for the liquid phase and a less-dominant bed load transport model for the solid phase. The resulting vertical grain size distributions in the debris flow deposits probably vary gradually from the finer particles (i.e. clay, silt, sand) of the liquid phase in the surface layer to the coarser particles (i.e. gravel, cobbles, boulders) of the solid phase in the lower layer. This is typically referred to as the normal distribution of graded bedding texture (see Figure 10 normal grading). On the other hand, if the liquid and solid phases are equally dominant [i.e. $U_l \approx U_s$, in scenario (ii)], then the uniform mobility of all grain sizes within the debris flow could potentially result in the formation of a vertically well-mixed deposit (Figure 10 mixing grading). In a rare situation, for the non-homogeneous debris flows with $U_l < U_s$ [i.e. scenario (iii)], the very high bulk density γ_m within such flows could provide strong buoyancy forces to support even the coarsest particles in suspension (Ancey, 2001), thus resulting in an inverse vertical distribution profile with the coarser-sized particles of the solid phase in the surface layer while finer-sized particles of the liquid phase in the lower layer of the debris deposits (see Figure 10 inverse grading). This scenario is relatively uncommon, but has been observed in the present studies (e.g., in Table 1).

Similar observations of inverse grading within the debris-flow deposits have also been made by Major (1994; 1997) in a large debris flow flume, which is to some extent different from the present study owing to: (i) *en masse* sediment emplacement was generally observed from

a single surge formed by the multiple surges as the debris flow typically adjusted in the transition zone (see Figure 2) with milder slope and wider transverse section; and (ii) viscous debris flows were commonly developed within the present experiment, which differed from the cohesionless mixtures used by Major (1994; 1997) aiming to avoid the mechanical influence of the cohesion. Despite our observations failed to recover a debris-flow event from its transportation to deposition, the present study can still faithfully correlate the flow behaviour with the depositional process because all the experimental debris flows were created in the same channel (with similar materials as well). Although many phenomenological (e.g. Fan and Hill, 2011; Ancey et al., 2011), as well as physically-based studies (e.g. Larcher and Jenkins, 2015) were performed to investigate the particle segregation dynamics, they were less supportive to explain the three different vertical grading patterns observed from the debris-flow deposits because: (i) these studies have been conducted to focus on the granular flows devoid of the liquid phase (and fine particles), which is obviously different from the debris flows; (ii) their granular flow was a binary mixture composed of two uniform size particles, which could not represent more complex grain size compositions of the debris flow; (iii) the initial configuration with two singletons were sometimes well designed, which could not reflect more realistic debris-flow field environments; and (iv) they were more concerned on the particle segregation and cluster patterns rather than the vertical grading features associated with the debris-flow deposits discussed herein.

5.3 Rheological behaviour of finer materials

The flow curve of all finer materials used in the experimental debris flows is shown in Figure 13. It is clear that all the investigated finer materials behave like a non-Newtonian fluid, namely the flow suddenly initiates at a relatively high shear stress value (O'Brien and Julien, 1988; Davies et al., 1992; Armanini et al., 2005; Santolo et al., 2010; Takahashi, 1991, 2014). Moreover, to attain the same shear rate, a higher shear stress would be required for the mixture with an increasing solid volumetric concentration, as implicitly indicated by the liquid-phase C_{vf} in Fig. 13. However, this rheological approach could be generally adopted to treat the debris-flows as one single phase (Santolo et al., 2010), and thus would not be

appropriate for the case of non-homogenous debris flows in the present study. Again, it should be emphasized that only the mixtures finer than 2.0 mm were allowed for the rheological tests owning to the limitations of the experimental equipment. Obviously, this type of mixture is neither liquid phase nor solid phase as specified on the basis of critical grain size d_0 (≈ 4.7 – 7.0 mm) in this work. Thus, the rheological parameters determined by this finer material of limited grain size using a conventional rheometer should not represent either the bulk rheological behaviour of the complete debris-flow materials (Santolo et al., 2010) or the behaviour of single liquid/solid phase within the non-homogeneous debris flows. In this sense, further relevant tests would be necessary in which we should consider: (i) how to determine the critical grain size d_0; and (ii) how to conduct the rheological experiments for the liquid/solid phase or bulk mixture through a new type of rheological equipment without the grain-size restriction.

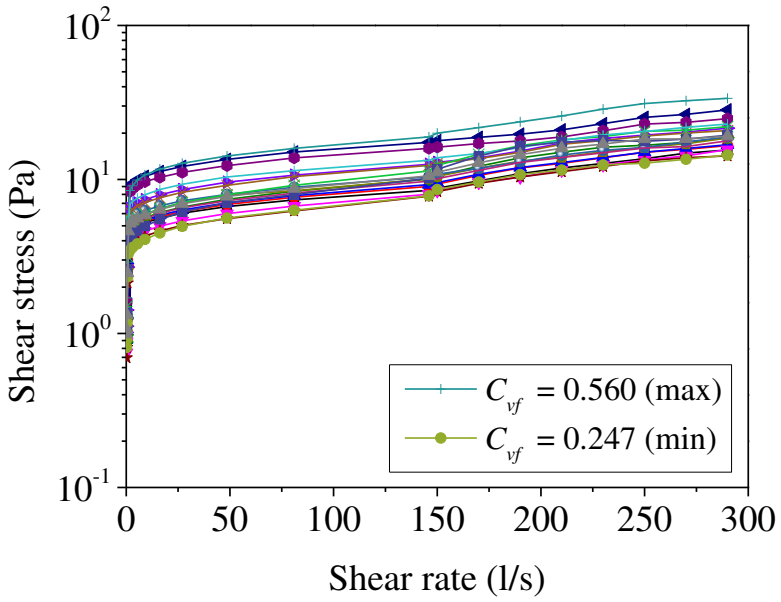

Figure 13: Flow curve of the finer materials in experimental debris flows (materials truncated at d_{max} = 2.0 mm for all the rheological tests)

6. Conclusions

In this paper we carried out extensive experimental and field observations on the non-homogeneous, two-phase debris flows at the Jiangjia gully, Yunnan Province of China. Through the theoretical analysis, we have derived the critical grain diameter between the solid and liquid phases of the debris flow through the principle of minimum energy dissipation. Based on this, the equations of two-phase velocities have been given and the dynamic inter-phase relationships have been explored. Further, a suggestive correspondence has been obtained between the point at which the calculated differences between the solid and fluid velocities cross zero and a change in the observed grading patterns within the same experimental gully. The results show that for the majority of debris flows investigated in the study, they were mainly dominated by the liquid phase. Correspondingly, the fine particles of the liquid phase and coarse particles of the solid phase were distributed in the upper and lower layers, respectively, within the resulting deposits. However, as the bulk density of the debris flow increases, the solid phase could have a higher velocity than the liquid one. Accordingly, more coarse particles are presumably transported as the suspended load and thus deposited on the upper layer, forming an unusual inverse vertical grain size distribution. In between, where the liquid and solid phases demonstrate equivalent transport velocities, the extensive exchange of fine and coarse particles in the non-homogeneous debris flows may result in a well-mixed grading pattern. Finally, the comparison between the calculated and measured velocities suggests that a reasonable agreement has been achieved.

It should be acknowledged here that the predicted two-phase velocities cannot be verified presently because no experimental measurements of real velocities of the liquid and solid phase during the debris-flow transport are available. We have acknowledged this as limitations of our present study and proposed this to be future work with the aid of more advanced technology. Also vigorous attempts should be made to scale the results for generality on the practical debris flow disaster predictions.

Acknowledgements

Special thanks should go to the support and help from Dongchuan Debris Flow Observation and Research Station, Chinese Academy of Sciences (CAS). The study is supported by the National Natural Science Foundation of China (Grant No. 11372048), National Basic Research Program of China (Grant No. 2011CB403304, 2013CB036402), Open Fund of the Key Laboratory of Mountain Hazards and Earth-surface Processes of CAS. Special thanks are also extended to Dr Alan Cuthbertson, Associate Professor from Heriot-Watt University, for his invaluable comments during the preparation of the manuscript.

Appendix

1. Liquid-phase velocity

According to the previous definition of the critical diameter d_0, the liquid and solid phases in a non-homogeneous debris flow can be quantitatively separated. The average stream-wise velocity for the liquid phase (i.e. $d < d_0$, in suspension) can be expressed in terms of the Darcy-Weisbach equation (Chow, 1959) as follows:

$$U = \sqrt{\frac{8gRJ_l}{f_m}} = \sqrt{\frac{8}{f_m}} \cdot u_* \tag{A1}$$

where $u_* = (gRJ_l)^{1/2}$ is the frictional velocity; and f_m is the Darcy-Weisbach frictional factor of the debris-flow mixture, which was empirically specified by Fei (1991) as

$$f_m = 0.11\beta\left(\frac{d_0}{4R} + \frac{68}{R_{em}}\right)^{1/4} \tag{A2}$$

where β is the drag reduction coefficient ($\beta = 0.82 - 0.95$); and R_{em} is the Reynolds number and determined by the liquid velocity U_l. By adopting a trial and error approach, the Darcy coefficient f_m was shown to vary only within a small range (i.e. $f_m = 0.019 - 0.024$). Experimental

results of Fei & Shu (2004) indicated that when the suspended load within a debris flow reaches the equilibrium state [Note: (i) the experiments were conducted in a 16 m long, 0.5 m wide and 0.5 m deep flume; (ii) natural sediment was employed in the experiment with bulk density γ_s = 2.65 t/m^3 and sediment size of 0.0016 – 0.40 mm; and (iii) the concentration C varied between 40 – 760 kg/m^3], the non-dimensional settling parameter ω/u_* could be empirically defined as

$$\frac{\omega}{u_*} = 0.036\left[S_v \left(\frac{4R}{d_{90}} \right)^{1/6} \right]^{-2/3} \tag{A3}$$

where d_{90} can be regarded as the maximum particle diameter in the liquid phase. It should be clarified that the critical diameter d_0 proposed to separate the liquid (consisting of the fine particles and water) and solid phases (consisting of the coarse particles) within a non-homogeneous debris flow, is theoretically larger than the maximum particle diameter in the liquid phase and smaller than the minimum particle diameter in the solid phase by definition. However, the maximum particle diameter in the liquid phase (and the minimum particle diameter in the solid phase) is practically close to the critical grain diameter d_0. Therefore, it can be reasonably assumed that the liquid phase related to $d_{90} \approx d_0$. Substituting Eq. (A3) into Eq. (A1), the velocity of the liquid phase can therefore be theoretically given by

$$U_l = 27.8\sqrt{\frac{8}{f_m}}\omega_0 \cdot S_{vf}^{2/3}\left(\frac{4R}{d_0} \right)^{\frac{1}{9}} \tag{A4}$$

2. Solid-phase velocity

In a two-dimensional debris flow, the discharge per unit width q is defined as the product of the mean velocity U_0 and the flow depth h. By taking the volumetric concentration of the solid phase C_{vc} into consideration, the liquid-phase flow discharge can be expressed as

$$q(1-C_{vc}) = U_l\left[h - h'(1-C_{vc}) \right] \tag{A5}$$

where h' is the flow depth corresponding to the solid phase of the debris flow (under the condition of so-called "limited" concentration C_{vm} (or maximum packing concentration), as indicated in Figure A1). This limited concentration C_{vm} arises due to the wide range of

particle sizes contained within the non-homogeneous debris flows, which results in the interstitial filling effect of fine particles (in the liquid phase) with the coarse grains (in the solid phase). The limited concentration was also empirically defined by Fei (1991) using data analysis as follows:

$$C_{vm} = 0.92 - 0.2 \lg \sum_{i=1}^{n} \frac{\Delta p_i}{d_i} \tag{A6}$$

where d_i and Δp_i represent the specific grain size and related weight proportion, respectively (Again, the limited concentration C_{vm} was neither calibrated nor adjusted in any way using the measured debris flow velocities U_0 in present study, and C_{vm} = 0.635 – 0.887 was simply taken for the experimental and natural debris flows). On the basis of this, the following mass-conservation relations of the solid phase (see Figure A1) can be defined

$$qC_{vc} = h'U_s \tag{A7a}$$

$$hC_{vc} = C_{vm}h' \tag{A7b}$$

The solid phase velocity in a non-homogeneous debris flow can thus be theoretically derived by substituting C_{vc} and C_{vm} for h and h' [from Eq. (A6)] into Eq. (A5), such that

$$U_s = U_l\left(\frac{C_{vm}}{1 - C_{vc}} - C_{vc}\right) \tag{A8}$$

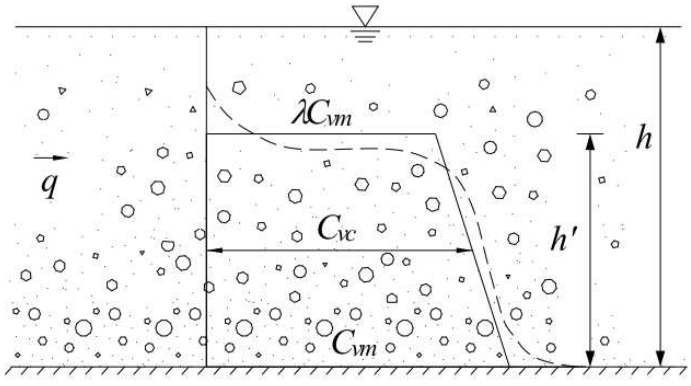

Figure A1: Schematic diagram of non-homogeneous debris flow concentration distribution

References

Armanini, A., Capart, H., Fraccarollo, L. and Larcher, M., 2005. Rheological stratification in experimental free-surface flows of granular–liquid mixtures. *Journal of Fluid Mechanics*, 532:269-319.

Armanini, A., Fraccarollo, L., and Rosatti, G., 2009. Two-dimensional simulation of debris flows in erodible channels. *Computers & Geosciences*, 35(5):993-1006.

Armanini. A., Larcher. M., Nucci. E., Dumbser. M., 2014. Submerged granular channel flows driven by gravity. Advances in Water Resources, 63: 1-10.

Ancey, C., 2001. 21 Debris Flows and Related Phenomena. In *Geomorphological Fluid Mechanics*. Springer, Berlin Heidelberg.

Ancey. C., Gray, J., Bustamante. S., et al., 2011. Experimental investigation of a breaking size segregation wave in a dry granular flow. *Aci Structural Journal*.

Bagnold, R.A., 1954. Experiments on a gravity free dispersion on large solid spheres in a Newtonian fluid under shear. *Proceedings of the Royal Society of London*, Series A, 225: 49-63.

Cheng, N.S., Cui, P., Liu, Z.G., Wei, F.Q., 2003. Calculation of the debris flow concentration based on clay content. *Science in China Series E*, 46:163-174.

Chow, V. T., 1959. Open-channel Hydraulics. McGraw-Hill, New York.

Cui, P., Chen, X.Q., Wang, Y.Y., Hu, K.H., Li, Y., 2005. JiangJia Ravine debris flows in south-western China. *Debris-flow Hazards and Related Phenomena*, Springer, 565-594.

Davies, T., Phillips, C., Pearce, A. et al., 1992. Debris flow behavior - an integrated overview, IAHS Publ, 209(21): 225.

Fan, Y., Hill, K. M., 2011. Phase transitions in shear-induced segregation of granular materials. *Physical Review Letters*, 106(21):2189-2192.

Fei, X.J., Shu A.P., 2004. Movement Mechanism and Disaster Control for Debris Flow. Tsinghua University Press, Beijing (in Chinese).

Fraccarollo, L., Papa, M., 2000. Numerical simulation of real debris-flow events. *Physics and Chemistry of the Earth, Part B: Hydrology, Oceans and Atmosphere*, 25(9): 757-763.

Hungr, O., 1995. A model for the runout analysis of rapid flow slides, debris flows and

avalanches. *Canadian Geotechnical Journal*, 32(4): 610-623.

Iverson, R.M., 1997a. The physics of debris flows. *Reviews of Geophysics*, 35: 245-296.

Iverson, R.M., 1997b. Hydraulic modeling of unsteady debris-flow surges with solid-liquid interactions. *Debris-Flow Hazards Mitigation: Mechanics, Prediction and Assessment, Proceedings of the First International Conference*, ASCE, New York, 550-560.

Iverson, R. M., Reid, M. E., LaHusen, R. G., 1997c. Debris-flow mobilization from landslides 1. *Annual Review of Earth and Planetary Sciences*, 25(1): 85-138.

Iverson, R.M., Vallance, J.W., 2001. New views of granular mass flows. *Geology*, 29(2): 115-118.

Kang, Z.C., Cui, P., Wei, F.Q., 2006. Data Collection of Dongchuan Debris Flow Observation and Research Station. Science Press, Beijing (in Chinese).

Lai, C., 1991. Modelling alluvial channel flow by multimode characteristic method. *Journal of Engineering Mechanics*, 117(1): 32-53.

Larcher, M., Jenkins, J. T., 2015. The evolution of segregation in dense inclined flows of binary mixtures of spheres. *Journal of Fluid Mechanics*, 782:405-429.

Liu, J.J., Li Y., Su P.C., Cheng Z.L., Cui P., (2009) Temporal variation of intermittent surges of debris flow. *Journal of Hydrology*, 365(3-4):322-328.

Major, J.J., Pierson, T.C., 1992. Debris flow rheology: experimental analysis of fine-grained slurries. *Water Resources Research*, 28: 841-857.

Major, J.J., 1994. Experimental studies of deposition at a debris flow flume. US Geological Survey Fact Sheet, 28.

Major, J.J., 1997. Depositional processes in large-scale debris-flow experiments. *Journal of Geology*, 105: 345–66.

Martinez, C.E., 2009. Eulerian-Lagrangian Two Phase Debris Flow Model. PhD Thesis, Florida International University.

Montgomery, D. R. and Dietrich, W. E., 1994. A physically based model for the topographic control of shallow landsliding. *Water Resource Research*, 30:1153-1171.

Naylor, M.A., 1980. The origin of inverse grading in muddy debris flow deposits - a review. *Journal of Sedimentary Research*, 50(4):1111-1116.

O'Brien, J. S., Julien, P. Y., 1985. Physical processes of hyperconcentrated sediment flows, in:

Proc. of the ASCE Specialty Conference on the Delineation of Landslides, Floods, and Debris Flow Hazards in Utah, Utah Water Research Laboratory, Series UWRL/g-85/03, 260-279.

O'Brien, J. S., Julien, P. Y., 1988. Laboratory analysis of mudflow properties, *Journal of Hydraulic Engineering*, 114(8):877-887.

Patra, A.K., Bauer, A.C., Nichita, C.C., Pitman, E.B., Sheridan, M.F., Bursik, M., Rupp, B., Webber, A., Stinton, A.J., Namikawa, L.M., 2005. Parallel adaptive numerical simulation of dry avalanches over natural terrain. *Journal of Volcanology and Geothermal Research*, 139(1): 1-21.

Pitman, E.B., Le, L., 2005. A two-fluid model for avalanche and debris flows. *Philosophical Transactions of the Royal Society*, 363(1832):1573-1601.

Rickenmann, D., Laigle, D.M.B.W., McArdell, B.W., Hübl, J., 2006. Comparison of 2D debris-flow simulation models with field events. *Computational Geosciences*, 10(2): 241-264.

Rosatti, G., Zorzi, N., Begnudelli, L., and Armanini, A., 2015. Evaluation of the Trent2D model capabilities to reproduce and forecast debris-flow deposition patterns through a back analysis of a real event, *Engineering Geology for Society and Territory*, 2, 1629-1633.

Santolo, A.S.D., Pellegrino, A.M., Evangelista, A., 2010. Experimental study on the rheological behaviour of debris flow. *Natural Hazards & Earth System Science*, 10: 2507-2514.

Savage, S.B., Hutter, K., 1989. The motion of a finite mass of granular material down a rough incline. *Journal of Fluid Mechanics*, 199(1):177-215.

Sheridan, M.F., Stinton, A.J., Patra, A., Pitman, E.B., Bauer, A., Nichita, C.C., 2005. Evaluating Titan2D mass-flow model using the 1963 Little Tahoma Peak avalanches, Mount Rainier, Washington. *Journal of Volcanology and Geothermal Research*, 139(1): 89-102.

Shu, A. P., Fei, X. J., Feng, Y. 2007. A preliminary study on energy dissipating mechanism for viscous debris flow. 4th International Conference on Debris-Flow Hazards Mitigation: Mechanics, Prediction, and Assessment, Chengdu, 131-137.

Shu, A.P., Zhang, Z.D., Wang, L., Fei, X.J., 2008. Method for determining the critical grain size of viscous debris flow based on energy dissipation principle. *Journal of Hydraulic Engineering*, 38(3): 257-263(in Chinese).

Shu, A.P., Wang, L., Yang, K., Fei, X.J., 2010. Investigation on movement characteristics for non-homogeneous and solid-liquid two-phase debris flow. *Science China Bulletin*, 55(30): 3006-3012 (in Chinese).

Stancanelli, L.M., Foti, E., 2015. A comparative assessment of two different debris flow propagation approaches–blind simulations on a real debris flow event. *Natural Hazards and Earth System Sciences*, 15(4): 735-746.

Starheim, C.C.A., Gomez, C., Harrison, J., Kain, C., Brewer, N.J., Owen, K., 2013. Complex internal architecture of a debris-flow deposit revealed using ground-penetrating radar, Cass, New Zealand. *New Zealand Geographer*, 69(1): 26-38.

Suwa, H., Okuda, S., 1983. Deposition of debris flows on a fan surface, Mt. Yakedake, Japan: Zeits. *Geomorphologie*, Suppl. Band 46: 79-101.

Takahashi, T., 1978. Mechanical characteristics of debris flow. *Journal of the Hydraulics Division*, HY8: 1153-1169.

Takahashi, T., 1980. Debris flow on prismatic open channel. *Journal of Hydraulics Division*, HY3: 381-396.

Takahashi, T., 1991. Debris flow: Monograph of IAHR, Balkema, Rotterdam: 1-165.

Takahashi, T., 2007. Debris flow: mechanics, prediction and countermeasures, Taylor and Francis: 1-102.

Takahashi, T., 2014. Debris flow: mechanics, prediction and countermeasures: CRC press.

Wang, Y.Y., Tan, R.Z., Jan, C.D., Tian, B., 2009. Gravel accumulation in deposits of viscous debris flows with hyper-concentration. *Journal of Mountain Science*, 6(1): 88-95.

Wang, Z., Qian, N., 1987. Laminated load: its development and mechanism of motion. *International Journal of Sediment Research*, 2(1):102-124.

Williams, R., Stinton, A.J., Sheridan, M.F., 2008. Evaluation of the Titan2D two-phase flow model using an actual event: case study of the 2005 Vazcun Valley lahar. *Journal of Volcanology and Geothermal Research*, 177(4): 760-766.

Wu J. S., Tian L. Q., Kang Z. C., Zhang S. C., Liu J. 1993. Debris flow and its

comprehensive control. Science Press, Beijing (in Chinese).

Xiong, G., 1996. Mechanism of Viscous Debris Flow. PhD Thesis, Tsinghua University, Beijing (in Chinese).

Yang, H.J., Wei, F.Q., Hu, K.H., Wang, C.C., 2014. Determination of the suspension competence of debris flows based on particle size analysis. *International Journal of Sediment Research*, 29(1): 73-81.